

Global fits in the Georgi-Machacek model

Cheng-Wei Chiang,^{1,2,*} Giovanna Cottin,^{1,†} and Otto Eberhardt^{3,‡}

¹*Department of Physics, National Taiwan University, Taipei 10617, Taiwan*

²*Institute of Physics, Academia Sinica, Taipei 11529, Taiwan*

³*IFIC, Universitat de València - Consejo Superior de Investigaciones Científicas,
Apt. Correus 22085, E-46071, València, Spain*

(Dated: October 1, 2022)

Abstract

Off the beaten track of scalar singlet and doublet extensions of the Standard Model, triplets combine an interesting LHC phenomenology with an explanation for neutrino masses. The Georgi-Machacek model falls into this category, but it has never been fully explored in a global fit. We use the `HEPfit` package to combine recent experimental Higgs data with theoretical constraints and obtain strong limits on the mixing angles and mass differences between the heavy new scalars as well as their decay widths. We also find that the current signal strength measurements allow for a Higgs to vector boson coupling with an opposite sign to the Standard Model, but this possibility can be ruled out by the lack of direct evidence for heavy Higgs states. For these hypothetical particles, we identify the dominant decay channels and extract bounds on their branching ratios from the global fit, which can be used to single out the decay patterns relevant for the experimental searches.

* chengwei@phys.ntu.edu.tw

† gcottin@phys.ntu.edu.tw

‡ otto.eberhardt@ific.uv.es

I. INTRODUCTION

The discovery of a new scalar resonance at the LHC [1, 2], consistent with the Higgs boson of the Standard Model (SM), confirms its particle content. Still several experimental observations, such as data on neutrino oscillations [3], beg for new physics explanations, whose effects are actively being looked for by the LHC experiments.

Among the well-motivated directions for new physics beyond the SM is the presence of an extended Higgs sector, which can lead to richer Higgs phenomenology at colliders. One possibility is the existence of additional Higgs triplet representations of $SU(2)$, in which neutrino masses can arise from the interaction of the SM Higgs doublet with the triplet field, that acquires a vacuum expectation value (VEV) v_Δ after electroweak symmetry breakdown (EWSB). Particularly in order to avoid conflicts with the electroweak ρ parameter [3], the Georgi-Machacek (GM) model [4, 5] adds one complex and one real scalar triplet in a way that ensures custodial $SU(2)_V$ symmetry is preserved in the scalar potential after the EWSB. The model predicts the existence of several Higgs multiplets, whose mass eigenstates form a quintet (H_5), one triplet (H_3) and two singlets (H_1 and h) under the custodial symmetry. In this work, we denote the 125-GeV Higgs boson by h .

The rich Higgs particle spectrum and associated attractive phenomenology deserve in-depth studies, as it is of crucial importance to understand to which extent there is still room for new physics in the Higgs sector. Notably, if v_Δ is sufficiently large, we can have enhanced couplings between the SM-like Higgs boson and the weak gauge bosons. For example, $\kappa_W = 1.28^{+0.18}_{-0.17}$ is reported in a recent measurement by the CMS Collaboration [6], giving a hint for us to consider a Higgs sector with larger field representations [7, 8]. The GM model serves as a minimal model with this feature. Modifications to the SM-like Higgs couplings with other particles can be probed by precise determination of the Higgs signal strengths at the LHC. Aside from loop-mediated processes, such data can constrain v_Δ and the mixing angle between the singlets α without the need to specify the heavy Higgs masses. In view of expected high precision in determining the Higgs couplings to other SM particles, Refs. [9, 10] recently even computed the renormalized κ factors, defined to be Higgs couplings in the model normalized to their corresponding SM values, at the one-loop level. Since H_1 and h are related via an orthogonal rotation, these signal strengths also provide significant constraints on the couplings of H_1 to SM particles.

Earlier studies had shown various collider constraints on the parameter space of the GM model [8, 11–17]. In Ref. [15], for example, it was shown that after considering theoretical bounds (namely, the stability of the potential and perturbative unitarity at tree level), the LHC Higgs signal strengths, together with electroweak precision observables, a favored region in the (v_Δ, α) plane is chosen by the data.

In this work, we go beyond the existing literature by performing global parameter fits in the GM model, including up-to-date experimental results from Run 1 and Run 2 of the LHC, by making use of the **HEPfit** open-source package [18]. This approach is in stark contrast to studies that only examine specific benchmark scenarios (that may miss interesting possibilities), as all the model parameters are varied simultaneously in the fits and a model likelihood is obtained. The package also allows the possibility to identify which of the experimental data impose most stringent bounds.

This paper is organized as follows. We start with a brief review of the GM model in Sec. II. Theoretical constraints on the scalar potential stability and perturbative unitarity at tree level are also included in our fits, as described in Sec. IV A. We then consider all

available experimental data on Higgs boson signal strengths in Sec. IV B, including the $\gamma\gamma$ mode, thus extending the considerations in Ref. [15]. Constraints from sixty-seven heavy Higgs direct searches at the LHC as well as the basics of `HEPfit` package are described in Sec. IV C. They are included in our Bayesian analysis, and greatly extend the amount of constraints analyzed in previous works [12, 14, 15]. Combined results of the fits and discussions are presented in Sec. V. We close the paper with a summary of our findings in Sec. VI.

II. THE GEORGI-MACHACEK MODEL

In the GM model [4, 5], $SU(2)$ -triplet complex scalar χ and real scalar ξ are added to the SM particle content. Assuming that the custodial symmetry is preserved at tree level, we can write the SM doublet and new triplet scalar fields as a bi-doublet and a bi-triplet, respectively,

$$\Phi = \begin{pmatrix} (\phi^0)^* & \phi^+ \\ -(\phi^+)^* & \phi^0 \end{pmatrix}, \quad \Delta = \begin{pmatrix} (\chi^0)^* & \xi^+ & \chi^{++} \\ -(\chi^+)^* & \xi^0 & \chi^+ \\ (\chi^{++})^* & -(\xi^+)^* & \chi^0 \end{pmatrix}.$$

After EWSB, the scalar fields have the VEV's given by

$$\langle \Phi \rangle = \frac{v_\Phi}{\sqrt{2}} \mathbb{1}_{2 \times 2} \quad \text{and} \quad \langle \Delta \rangle = v_\Delta \mathbb{1}_{3 \times 3} \quad (1)$$

Using, the above-defined fields, the scalar potential

$$\begin{aligned} V(\Phi, \Delta) = & \frac{1}{2} m_\Phi^2 \text{tr} [\Phi^\dagger \Phi] + \frac{1}{2} m_\Delta^2 \text{tr} [\Delta^\dagger \Delta] + \lambda_1 (\text{tr} [\Phi^\dagger \Phi])^2 + \lambda_2 (\text{tr} [\Delta^\dagger \Delta])^2 \\ & + \lambda_3 \text{tr} [(\Delta^\dagger \Delta)^2] + \lambda_4 \text{tr} [\Phi^\dagger \Phi] \text{tr} [\Delta^\dagger \Delta] + \lambda_5 \text{tr} \left[\Phi^\dagger \frac{\sigma^a}{2} \Phi \frac{\sigma^b}{2} \right] \text{tr} [\Delta^\dagger T^a \Delta T^b] \\ & + \mu_1 \text{tr} \left[\Phi^\dagger \frac{\sigma^a}{2} \Phi \frac{\sigma^b}{2} \right] (P^\dagger \Delta P)_{ab} + \mu_2 \text{tr} [\Delta^\dagger T^a \Delta T^b] (P^\dagger \Delta P)_{ab}, \end{aligned} \quad (2)$$

where σ^a are the Pauli matrices, T^a are the 3×3 matrix representation of the $SU(2)$ generators, and the similarity transformation relating the $SU(2)$ generators in the triplet and adjoint representations is given by

$$P = \frac{1}{\sqrt{2}} \begin{pmatrix} -1 & i & 0 \\ 0 & 0 & \sqrt{2} \\ 1 & i & 0 \end{pmatrix}.$$

Note that the triplet VEV is induced by the SM EWSB via the μ_1 interaction.

Under the custodial $SU(2)_V$ symmetry, the physical eigenstates can be written as a quintet $H_5 = (H_5^{++}, H_5^+, H_5^0, H_5^-, H_5^{--})^T$ with mass m_5 , a triplet $H_3 = (H_3^+, H_3^0, H_3^-)^T$ with mass m_3 and two scalar singlets H_1 and h , of which the former has the mass m_1 and the latter is identified with the 125-GeV scalar boson found at the LHC. The relations between the physical fields and the original fields can be found in, for example, Ref. [11]. Rotating from the original basis to the mass basis involves two mixing angles α and β , where α diagonalizes

the singlet subspace and $\tan \beta \equiv v_\Phi/(2\sqrt{2}v_\Delta)$ is used in the diagonalization of the Goldstone modes and the physical triplet states. In the limit of custodial symmetry, the states in each of the above-mentioned representations are degenerate in mass. An $\mathcal{O}(100)$ MeV mass splitting is expected among the states within the same representation because of custodial symmetry breaking by hypercharge interactions. In this article, we assume that h is the lightest scalar boson in the GM Higgs spectrum.

We list a few remarkable features of the GM model here. First, the hWW and hZZ couplings can be larger than the SM values at tree level. This does not happen in models extended with only singlet and/or doublet scalars. This feature is resistant to loop corrections, as explicitly shown in Refs. [9, 10] at the one-loop level. Secondly, the quintet Higgs bosons have couplings with the weak gauge bosons, while the triplet Higgs bosons do not. The triplet Higgs bosons are thus said to be gauge-phobic. On the other hand, the triplet Higgs bosons have couplings with SM fermions, while the quintet Higgs bosons do not. The latter are thus said to be fermiophobic. Finally, the $H_5^0 ZZ$ coupling divided by the $H_5^0 WW$ coupling is -2 , while the corresponding ratios for h and H_1 are 1.

III. HEPFIT

The open-source package **HEPfit** is a multi-purpose tool to calculate many different high-energy physics observables and theory constraints in various models. It is interfaced with **BAT** [19] to perform Bayesian fits with Markov Chain Monte Carlo simulations. Here, we present the first results from the implementation of the GM model into **HEPfit**. The global fit allows us to scrutinize this model with unprecedented precision as it allows us to vary all GM parameters simultaneously, and thus guarantees that we do not miss important features when scanning over the parameter space. This method has also been used in the two-Higgs doublet model [20–22], and the GM implementation is partially based on the well-tested two-Higgs doublet model part of **HEPfit** in order to minimize possible sources of errors.

In our fits, we fix $m_h = 125.09$ GeV and $v = \sqrt{v_\Phi^2 + 8v_\Delta^2} \approx 246$ GeV and all other SM parameters to their best-fit values [23]. We use the following prior ranges for the remaining GM parameters:

$$\begin{aligned} 150 \text{ GeV} &\leq m_1, m_3, m_5 \leq 1000 \text{ GeV}, \\ 0 \text{ GeV} &\leq v_\Delta \leq 86 \text{ GeV}, \\ -90^\circ &\leq \alpha \leq 90^\circ, \\ -1000 \text{ GeV} &\leq \mu_1, \mu_2 \leq 1000 \text{ GeV}, \end{aligned}$$

where the masses m_1, m_3, m_5 of the H_1, H_3 and H_5 bosons, respectively, are chosen to be heavier than the 125 GeV Higgs and lighter than 1 TeV, as we want to cover the ranges that are interesting for the LHC searches of heavy scalars. Accordingly, we also limit the absolute values of the trilinear couplings μ_1 and μ_2 to be below 1 TeV.

Concerning the heavy masses m_1, m_3 and m_5 , our type of priors will depend on the set of constraints being used. For the direct searches, we will use flat mass priors, as the search limits depend on the masses linearly. As for the h signal strengths and the theory bounds, they depend on the squared masses. Therefore, we choose flat priors for m_1^2, m_3^2 and m_5^2 between $(150 \text{ GeV})^2$ and $(1000 \text{ GeV})^2$ in this case. In the global fit to all constraints, we

apply both types of priors in two separate fits and overlay both fits in the figures and for the extraction of the limits. (See also Appendix B of Ref. [21] for the same procedure in two-Higgs doublet model fits.)

IV. FIT CONSTRAINTS

In this section, we list the theoretical and experimental constraints imposed on the GM model parameter space in this analysis.

A. Theory constraints

We take into account two different sets of theoretical constraints: stability of the scalar potential and perturbative unitarity, both at tree level. Stability of the electroweak vacuum is imposed by requiring that the scalar potential be bounded from below, which places restrictions on the λ quartic couplings. We implement the constraints from Section 4 of Ref. [24].

Perturbative unitarity of the S -matrix of 2 scalars to 2 scalars scattering processes forces additional restrictions on the quartic couplings. We implement all seventeen constraints from the full S -matrix described in Ref. [25]. Here we take the stronger limits that the real part of the zeroth partial wave amplitude has an absolute value less than $1/2$.

While the theory constraints are defined in terms of the quartic couplings of the scalar potential in Eq. (2), the following experimental bounds constrain the physical masses and the couplings of the scalars.

B. Higgs signal strengths

For the signal strengths computation, the predicted SM Higgs production cross-section σ and total decay width Γ are dressed with scale factors. For the production modes $i = \text{ggF, VBF, Wh, Zh, tth}$ and the decay modes $f = ZZ, WW, \gamma\gamma, Z\gamma, \tau\tau, \mu\mu, b\bar{b}$, we define r_i and r_f to be respectively the ratios of the production cross section σ_i and the decay width Γ_f with respect to their corresponding SM values. Therefore, the production cross section times the branching ratio for a particular channel in the GM model is given by

$$(\sigma_i \cdot \mathcal{B}_f)_{\text{GM}} = (\sigma_i \cdot \mathcal{B}_f)_{\text{SM}} \cdot r_i \cdot r_f \cdot \frac{\Gamma_{\text{SM}}}{\Gamma_{\text{GM}}}, \quad (3)$$

with Γ_{SM} and Γ_{GM} being the total widths of the Higgs boson in the SM and the GM model, respectively.

To quantify the deviation of the GM model from the SM, the signal strength of a process $\mu_i^f = \mu_i \cdot \mu_f$ with the production channel i and the decay of h to an f final state is then defined as

$$\mu_i^f = \frac{r_i \cdot r_f}{\sum_{f'} r_{f'} \cdot \mathcal{B}_{\text{SM}}(h \rightarrow f')}. \quad (4)$$

Each signal strength is computed in the narrow-width approximation, and depends on the GM h couplings to all final states. The values for all couplings are cross-checked with the predictions in Ref. [26].

		$b\bar{b}$	WW	$\tau\tau$	ZZ	$\gamma\gamma$	$Z\gamma$	$\mu\mu$
	SM Br	57.5%	21.6%	6.3%	2.7%	2.3‰	1.6‰	0.2‰
ggF ₈	87.2%	–	[27, 28]	[29, 30]	[31, 32]	[33, 34]	[35]	[36]
ggF ₁₃	87.1%	–	[6, 37]	[38]	[39, 40]	[41, 42]	[43]	[44, 45]
VBF ₈	7.2%	–	[27, 28]	[29, 30]	[31, 32]	[33, 34]		
VBF ₁₃	7.4%	[46]	[6, 37]	[38]	[39, 40]	[41, 42]		
Vh ₈	5.1%	[47, 48]	[28, 49]	[29, 30]	[31, 32]	[33, 34]		
Vh ₁₃	4.4%	[50, 51]	[6, 52]	[38]	[39, 40]	[41, 42]		
tth ₈	0.6%	[53, 54]	–	–	[31, 32]	[33, 34]		
tth ₁₃	1.0%	[55–57]	[6, 58, 59]	[58, 59]	[39, 40, 58, 59]	[41, 42]		
Vh ₂		[60, 61]						
tth ₂		[60]						

$$0 < \hat{\sigma} < 0.5 \quad 0.5 \leq \hat{\sigma} \leq 1.0 \quad \hat{\sigma} > 1.0 \quad (\hat{\sigma} = \sigma_{\min}/w)$$

TABLE I. Higgs signal strength inputs used in our fits. The Higgs decays are listed in separate columns, with the corresponding SM branching ratios given in the second line. In lines three to twelve, we give all LHC and Tevatron references of the used signal strengths, ordered by production mechanism and \sqrt{s} . For the LHC, we indicate the share of Higgs production in pp collisions for each channel in the second column. The background colors of the table cells give an idea about how precise the strongest signal strength measurement in a particular category is at present: green cells contain results with an uncertainty of less than 0.5 on μ , yellow cells have an uncertainty between 0.5 and 1, and red entries have not been measured with a precision smaller than 1 (see the text for more details). On the decays to $Z\gamma$ and $\mu\mu$, we only have information for pp production and assume the SM composition in the second column for them.

The experimental input values of the Higgs signal strengths are the same as in Ref. [62]. Instead of all ~ 130 numerical signal strength inputs, we show in Table I the current sensitivity of the individual channels, indicated by the background colors. The quantity $\hat{\sigma}$ is the ratio of the smallest uncertainty of all individual measurements in one table cell (σ_{\min}) and the weight of the corresponding production mechanism (w). For instance, in Ref. [38], we can find that $\mu^{\tau\tau} = 1.11^{+0.34}_{-0.35}$ in their VBF category, so $\sigma_{\min} = 0.34$ here. Note that the categories do not consist of only one production mechanism, and thus the given value is no measurement of $\mu^{\tau\tau}_{\text{VBF}}$. The admixture (weight) of VBF is only 57%, and so $\hat{\sigma} \approx 0.6$ in this case. We stress that $\hat{\sigma}$ depends on the *individual* measurements and not on the combination. It is only intended to give the reader a rough estimate of the achieved precision in every channel, and should not be understood as a quantitative statement. In the last two columns, we use the 8-TeV data from Ref. [35] ([43]) and the 13-TeV results from Ref. [43] ([44, 45]) for $Z\gamma$, since the only information about the initial state is the pp state rather than individual mechanisms.

Label	Channel	Experiment	Mass range [TeV]	\mathcal{L} [fb ⁻¹]
A_{13t}^{tt}	$tt \rightarrow \phi^0 \rightarrow tt$	ATLAS [63]	[0.4;1]	13.2
A_{13b}^{tt}	$bb \rightarrow \phi^0 \rightarrow tt$	ATLAS [63]	[0.4;1]	13.2
C_{8b}^{bb}	$bb \rightarrow \phi^0 \rightarrow bb$	CMS [64]	[0.1;0.9]	19.7
C_8^{bb}	$gg \rightarrow \phi^0 \rightarrow bb$	CMS [65]	[0.33;1.2]	19.7
C_{13}^{bb}	$pp \rightarrow \phi^0 \rightarrow bb$	CMS [66]	[0.55;1.2]	2.69
C_{13b}^{bb}	$bb \rightarrow \phi^0 \rightarrow bb$	CMS [67]	[0.3;1.3]	35.7
$A_8^{\tau\tau}$	$gg \rightarrow \phi^0 \rightarrow \tau\tau$	ATLAS [68]	[0.09;1]	20
$C_8^{\tau\tau}$		CMS [69]	[0.09;1]	19.7
$A_{8b}^{\tau\tau}$	$bb \rightarrow \phi^0 \rightarrow \tau\tau$	ATLAS [68]	[0.09;1]	20
$C_{8b}^{\tau\tau}$		CMS [69]	[0.09;1]	19.7
$A_{13}^{\tau\tau}$	$gg \rightarrow \phi^0 \rightarrow \tau\tau$	ATLAS [70]	[0.2;2.25]	36.1
$C_{13}^{\tau\tau}$		CMS [71]	[0.09;3.2]	35.9
$A_{13b}^{\tau\tau}$	$bb \rightarrow \phi^0 \rightarrow \tau\tau$	ATLAS [70]	[0.2;2.25]	36.1
$C_{13b}^{\tau\tau}$		CMS [71]	[0.09;3.2]	35.9
$A_8^{\gamma\gamma}$	$gg \rightarrow \phi^0 \rightarrow \gamma\gamma$	ATLAS [72]	[0.065;0.6]	20.3
$A_{13}^{\gamma\gamma}$	$pp \rightarrow \phi^0 \rightarrow \gamma\gamma$	ATLAS [73]	[0.2;2.7]	36.7
$C_{13}^{\gamma\gamma}$	$gg \rightarrow \phi^0 \rightarrow \gamma\gamma$	CMS [74]	[0.5;4]	35.9
$A_8^{Z\gamma}$	$pp \rightarrow \phi^0 \rightarrow Z\gamma \rightarrow (\ell\ell)\gamma$	ATLAS [75]	[0.2;1.6]	20.3
$C_8^{Z\gamma}$		CMS [76]	[0.2;1.2]	19.7
$A_{13}^{Z\gamma}$	$gg \rightarrow \phi^0 \rightarrow Z\gamma[\rightarrow (\ell\ell)\gamma]$	ATLAS [77]	[0.25;2.4]	36.1
$C_{8+13}^{Z\gamma}$	$gg \rightarrow \phi^0 \rightarrow Z\gamma$	CMS [78]	[0.35;4]	35.9
A_8^{ZZ}	$gg \rightarrow \phi^0 \rightarrow ZZ$	ATLAS [79]	[0.14;1]	20.3
A_{8V}^{ZZ}	$VV \rightarrow \phi^0 \rightarrow ZZ$	ATLAS [79]	[0.14;1]	20.3
$A_{13}^{2\ell 2L}$	$gg \rightarrow \phi^0 \rightarrow ZZ[\rightarrow (\ell\ell)(\ell\ell, \nu\nu)]$	ATLAS [80]	[0.2;1.2]	36.1
$A_{13V}^{2\ell 2L}$	$VV \rightarrow \phi^0 \rightarrow ZZ[\rightarrow (\ell\ell)(\ell\ell, \nu\nu)]$	ATLAS [80]	[0.2;1.2]	36.1
$A_{13}^{2L 2q}$	$gg \rightarrow \phi^0 \rightarrow ZZ[\rightarrow (\ell\ell, \nu\nu)(qq)]$	ATLAS [81]	[0.3;3]	36.1
$A_{13V}^{2L 2q}$	$VV \rightarrow \phi^0 \rightarrow ZZ[\rightarrow (\ell\ell, \nu\nu)(qq)]$	ATLAS [81]	[0.3;3]	36.1
$C_{13}^{2\ell 2X}$	$pp \rightarrow \phi^0 \rightarrow ZZ[\rightarrow (\ell\ell)(qq, \nu\nu, \ell\ell)]$	CMS [82]	[0.13;3]	35.9
A_8^{WW}	$gg \rightarrow \phi^0 \rightarrow WW$	ATLAS [83]	[0.3;1.5]	20.3
A_{8V}^{WW}	$VV \rightarrow \phi^0 \rightarrow WW$	ATLAS [83]	[0.3;1.5]	20.3
$A_{13}^{2(\ell\nu)}$	$gg \rightarrow \phi^0 \rightarrow WW[\rightarrow (e\nu)(\mu\nu)]$	ATLAS [84]	[0.25;4]	36.1
$A_{13V}^{2(\ell\nu)}$	$VV \rightarrow \phi^0 \rightarrow WW[\rightarrow (e\nu)(\mu\nu)]$	ATLAS [84]	[0.25;3]	36.1
$C_{13}^{2(\ell\nu)}$	$(gg+VV) \rightarrow \phi^0 \rightarrow WW \rightarrow (\ell\nu)(\ell\nu)$	CMS [85]	[0.2;1]	2.3
$A_{13}^{\ell\nu 2q}$	$gg \rightarrow \phi^0 \rightarrow WW[\rightarrow (\ell\nu)(qq)]$	ATLAS [86]	[0.3;3]	36.1
$A_{13V}^{\ell\nu 2q}$	$VV \rightarrow \phi^0 \rightarrow WW[\rightarrow (\ell\nu)(qq)]$	ATLAS [86]	[0.3;3]	36.1
C_8^{VV}	$pp \rightarrow \phi^0 \rightarrow VV$	CMS [87]	[0.145;1]	24.8

TABLE II. Neutral heavy Higgs boson searches at the LHC relevant for the neutral scalar in the GM model. $\phi^0 = H_1^0, H_3^0, H_5^0$. $V = W, Z$ and $\ell = e, \mu$.

Label	Channel	Experiment	Mass range [TeV]	\mathcal{L} [fb ⁻¹]
A_8^{hh}	$gg \rightarrow H_1^0 \rightarrow hh$	ATLAS [94]	[0.26;1]	20.3
C_8^{4b}	$pp \rightarrow H_1^0 \rightarrow hh \rightarrow (bb)(bb)$	CMS [95]	[0.27;1.1]	17.9
$C_8^{2\gamma 2b}$	$pp \rightarrow H_1^0 \rightarrow hh \rightarrow (bb)(\gamma\gamma)$	CMS [96]	[0.260;1.1]	19.7
$C_{8q}^{2b 2\tau}$	$gg \rightarrow H_1^0 \rightarrow hh[\rightarrow (bb)(\tau\tau)]$	CMS [97]	[0.26;0.35]	19.7
$C_8^{2b 2\tau}$	$pp \rightarrow H_1^0 \rightarrow hh[\rightarrow (bb)(\tau\tau)]$	CMS [98]	[0.35;1]	18.3
A_{13}^{4b}	$pp \rightarrow H_1^0 \rightarrow hh \rightarrow (bb)(bb)$	ATLAS [99]	[0.3;3]	13.3
C_{13}^{4b}		CMS [100]	[0.26;1.2]	35.9
$A_{13}^{2\gamma 2b}$	$pp \rightarrow H_1^0 \rightarrow hh[\rightarrow (bb)(\gamma\gamma)]$	ATLAS [101]	[0.275;0.4]	3.2
$C_{13}^{2\gamma 2b}$	$pp \rightarrow H_1^0 \rightarrow hh \rightarrow (bb)(\gamma\gamma)$	CMS [102]	[0.25;0.9]	35.9
$C_{13}^{2b 2\tau}$	$pp \rightarrow H_1^0 \rightarrow hh \rightarrow (bb)(\tau\tau)$	CMS [103]	[0.25;0.9]	35.9
$C_{13}^{2b 2V}$	$pp \rightarrow H_1^0 \rightarrow hh \rightarrow (bb)(VV \rightarrow \ell\nu\ell\nu)$	CMS [104]	[0.26;0.9]	35.9
$A_{13}^{2\gamma 2W}$	$gg \rightarrow H_1^0 \rightarrow hh[\rightarrow (\gamma\gamma)(WW)]$	ATLAS [105]	[0.25;0.5]	13.3
A_8^{bbZ}	$gg \rightarrow H_3^0 \rightarrow hZ \rightarrow (bb)Z$	ATLAS [106]	[0.22;1]	20.3
$C_8^{2b 2\ell}$	$gg \rightarrow H_3^0 \rightarrow hZ \rightarrow (bb)(\ell\ell)$	CMS [107]	[0.225;0.6]	19.7
$A_8^{\tau\tau Z}$	$gg \rightarrow H_3^0 \rightarrow hZ \rightarrow (\tau\tau)Z$	ATLAS [106]	[0.22;1]	20.3
$C_8^{2\tau 2\ell}$	$gg \rightarrow H_3^0 \rightarrow hZ \rightarrow (\tau\tau)(\ell\ell)$	CMS [97]	[0.22;0.35]	19.7
A_{13}^{bbZ}	$gg \rightarrow H_3^0 \rightarrow hZ \rightarrow (bb)Z$	ATLAS [108]	[0.2;2]	36.1
A_{13b}^{bbZ}	$b\bar{b} \rightarrow H_3^0 \rightarrow hZ \rightarrow (bb)Z$	ATLAS [108]	[0.2;2]	36.1
$C_8^{\phi Z}$	$pp \rightarrow \phi^0 \rightarrow \phi^{0'} Z \rightarrow (bb)(\ell\ell)$	CMS [109]	[0.13;1]	19.8

TABLE III. Neutral heavy Higgs boson searches at the LHC relevant for the neutral scalar in the GM model. $\phi^0 = H_1^0, H_3^0, H_5^0$ and $\ell = e, \mu$.

C. Searches for heavy Higgs particles

We consider a large variety of direct searches for heavy resonances performed by the ATLAS and CMS Collaborations in Run 1 and Run 2 of the LHC. Tables II and III summarize the experimental searches to date which can have sensitivity to the neutral scalars H_1^0 , H_3^0 and H_5^0 in the GM model. Table II shows all searches for a scalar resonance decaying into fermions or gauge bosons, and in Table III we list the cases with decays including one or two Higgs bosons. In Table IV, we list all searches for singly and doubly charged heavy scalars considered in our fits. Note that we are not sensitive in this model to the doubly charged Higgs searches in Refs. [88–90], where a 100% branching fraction to leptons is assumed and the decay of $H_5^{\pm\pm}$ to $W^\pm W^\pm$ is suppressed, a scenario quite contrary to what we are considering here. The ATLAS searches for a doubly charged Higgs in Refs. [91, 92] can have sensitivity in the two-lepton and three-lepton signal regions, and have been reinterpreted in the context of the Higgs triplet model [93] and GM model [14]. The limits provided by the experimental collaborations are not directly applicable to our case due to the $\mathcal{B}(H^{\pm\pm} \rightarrow \ell^\pm \ell^\pm) = 100\%$ assumption, and, since in this work we are not formally recasting these searches, we choose not to include them in the fits.

The analyses in Tables II, III and IV provide either model-independent 95% confidence level upper limits on the production cross-section times branching ratios, $\sigma \cdot \mathcal{B}$, for different

Label	Channel	Experiment	Mass range [TeV]	\mathcal{L} [fb ⁻¹]
$A_8^{\tau\nu}$	$pp \rightarrow H_3^\pm \rightarrow \tau^\pm \nu$	ATLAS [110]	[0.18;1]	19.5
$C_8^{\tau\nu}$	$pp \rightarrow H_3^+ \rightarrow \tau^+ \nu$	CMS [111]	[0.18;0.6]	19.7
$A_{13}^{\tau\nu}$	$pp \rightarrow H_3^\pm \rightarrow \tau^\pm \nu$	ATLAS [112]	[0.2;2]	14.7
$C_{13}^{\tau\nu}$		CMS [113]	[0.18;3]	12.9
A_8^{tb}	$pp \rightarrow H_3^\pm \rightarrow tb$	ATLAS [114]	[0.2;0.6]	20.3
C_8^{tb}	$pp \rightarrow H_3^+ \rightarrow t\bar{b}$	CMS [111]	[0.18;0.6]	19.7
A_{13}^{tb}	$pp \rightarrow H_3^+ \rightarrow t\bar{b}$	ATLAS [115]	[0.3;1]	13.2
A_{13}^{tb}		ATLAS [63]	[0.2;0.3]	13.2
A_8^{WZ}	$WZ \rightarrow H_5^\pm \rightarrow WZ[\rightarrow (qq)(\ell\ell)]$	ATLAS [116]	[0.2;1]	20.3
C_{13}^{WZ}	$WZ \rightarrow H_5^\pm \rightarrow WZ[\rightarrow (\ell\nu)(\ell\ell)]$	CMS [117]	[0.2;2]	15.2
$C_8^{\ell^\pm\ell^\pm}$	$VV \rightarrow H_5^{\pm\pm} \rightarrow W^\pm W^\pm[\rightarrow (\ell^\pm\nu)(\ell^\pm\nu)]$	CMS [118]	[0.2;0.8]	19.4
$C_{13}^{\ell^\pm\ell^\pm}$		CMS [119]	[0.2;1.0]	35.9

TABLE IV. Charged heavy Higgs boson searches at the LHC relevant for the singly and doubly charged scalars in the GM model. $V = W, Z$ and $\ell = e, \mu$.

production and decay modes, or they are quoted by $\sigma \cdot \mathcal{B}/(\sigma \cdot \mathcal{B})_{\text{SM}}$ as a function of the resonance mass. If the experimental result includes the branching ratio into a specific final state in the upper limit, we spell out the channel, using parentheses to combine particles which stem from a primary decay product. Whenever a secondary final state is written inside square brackets, it means that we are quoting the limit on the primary final state measured through that particular secondary final state.

In order to assess which parts of the GM model parameter space are favored after imposing these constraints, we first calculate the theoretical production cross-section times branching ratio, $\sigma \cdot \mathcal{B}$, for all modes. For the neutral H_1^0 , H_3^0 and singly charged H_3^\pm states, we calculate $\sigma \cdot \mathcal{B}$ taking inputs from the two-Higgs doublet model already implemented in `HEPfit` [20, 21], and rescale it to the GM model. We make use of the cross-section tables computed in Refs. [20, 21] and calculate all branching ratios taking inputs from the couplings defined in the Appendix of Ref. [120]. For the quintet, we make use of the 13- and 8-TeV production cross-section tables from the LHC Higgs Cross-Section Working Group [121], including VBF production cross-sections for $H_5^{\pm\pm}$, H_5^\pm , and H_5^0 . The remaining VH modes and pair production of doubly charged $H_5^{\pm\pm}$ are calculated with `MADGRAPH5_AMC@NLOv2.6.1` [122] at the leading order, taking the spectrum of the model generated with `GMCalc` [26] as input.

In order to compare the specific $\sigma \cdot \mathcal{B}$ (calculated in each case as above) with the experimental upper limit, we define a ratio for the theoretical value and the observed limit, to which we assign a Gaussian likelihood with zero central value, which is in agreement with the null results in the searches of heavy scalars so far.

V. RESULTS

Here we show the impact of all the constraints considered on the GM model. We first discuss the effect of the measured h signal strengths. In Figure 1, we show the individual

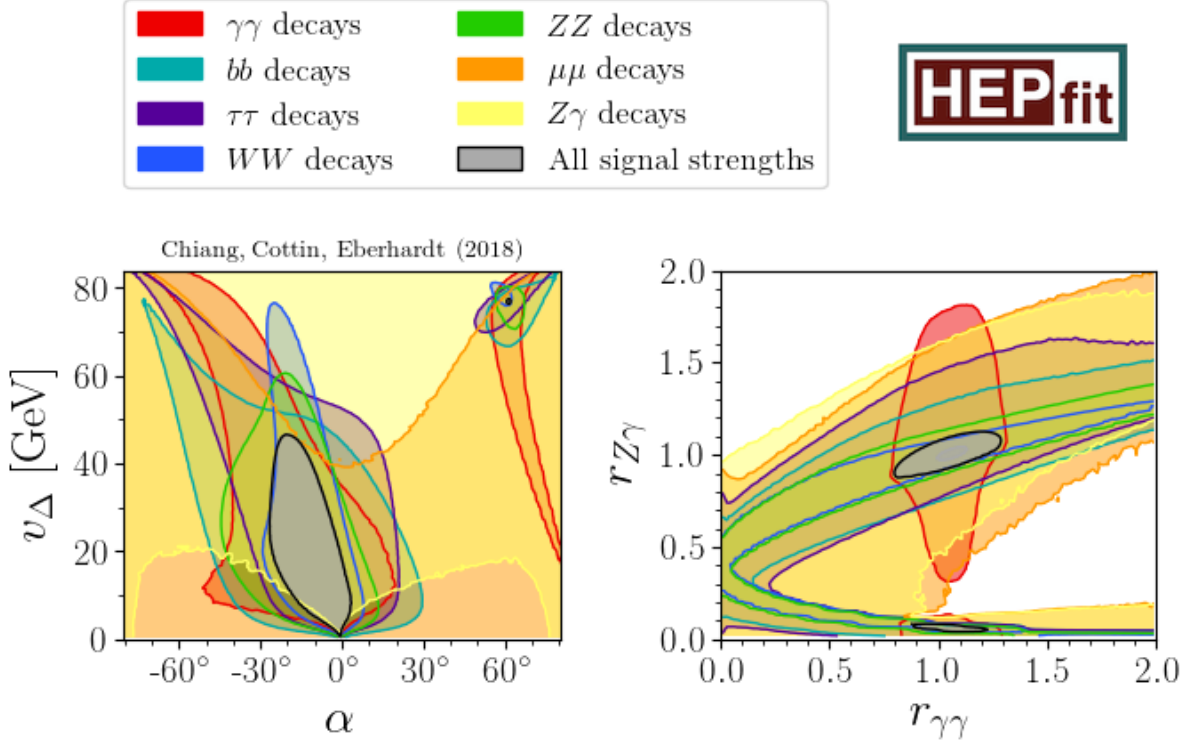


FIG. 1. Impacts of Higgs signal strengths on the v_Δ - α plane (left) and on the relative one-loop couplings of h to $\gamma\gamma$ and $Z\gamma$, $r_{\gamma\gamma}$ and $r_{Z\gamma}$, respectively (right). The 95% probability contours are shown from fits to the data for h decays to $\gamma\gamma$ (red), $Z\gamma$ (yellow), WW (blue), ZZ (green), bb (cyan), $\tau\tau$ (purple) and $\mu\mu$ (orange). The combined fit to all h signal strengths is shown in grey.

impacts of specific decay categories on the α - v_Δ plane and on the plane of the effective loop couplings of h to $\gamma\gamma$ and $Z\gamma$, as well as the combination of all signal strengths. While the colored contours represent the allowed regions with 95% probability for each decay mode, the grey region gives the combined fit.

Two allowed grey regions can be seen in the left panel of Figure 1. The bigger region close to $\alpha \approx 0^\circ$ (corresponding to the decoupling limit of the model) shows that v_Δ cannot exceed ≈ 50 GeV, and negative α is mostly favored. The other allowed solution close to $\alpha \approx 61^\circ$ and $v_\Delta \approx 77$ GeV features a negative sign for the h couplings to vector bosons relative to the SM ($r_{ZZ} = r_{WW} = -1$). This region was not identified before as a viable possibility in the GM model (see, for instance, Ref. [15]), highlighting the advantages of using a global fitter¹. The parameter space in the α - v_Δ plane is smaller in size as compared to the one given in Ref. [15], as now we see that α cannot reach beyond -30° . This is due to the much larger data set on h signal strengths made available in the recent years as well as the addition of the $\gamma\gamma$ signal strengths.

In the right panel of Figure 1, we show the probability contours in the $r_{Z\gamma}$ - $r_{\gamma\gamma}$ plane,

¹ Note that this region is visible only when considering the individual effects of the h signal strengths. It disappears after considering the effect of the direct searches (see Figure 2).

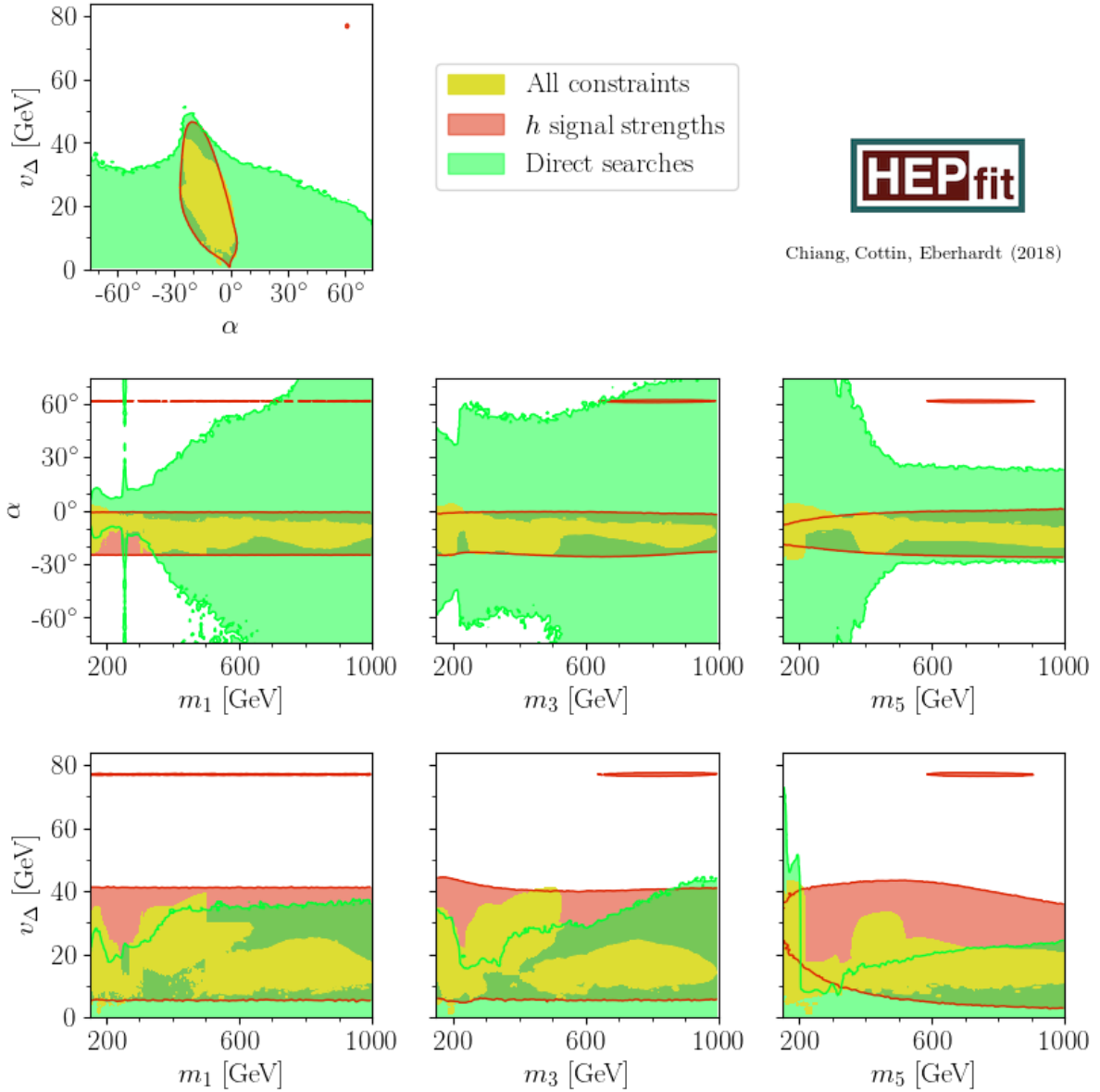


FIG. 2. Allowed 95% probability regions in the α vs. v_Δ , α vs. mass and v_Δ vs. mass planes. The red contour shows the effect of the h signal strengths, while in green we show the impact of the direct searches. The combined fit with all constraints is shown in yellow.

illustrating the impact on the one-loop couplings of h to $\gamma\gamma$ and $Z\gamma$ relative to the SM. The information on the loop couplings is complementary to the tree-level couplings, which can be purely determined for a given pair of α and v_Δ from the left panel. We observe a solution around the SM values, while a much smaller h coupling to $Z\gamma$ than the SM also remain to be allowed, since so far we only have upper limits on the $Z\gamma$ signal strength.

In Figure 2 we can see the effect of individual sets as well as all constraints in the v_Δ - α plane (top row), the α - $m_{1,3,5}$ plane (middle row), and v_Δ - $m_{1,3,5}$ plane (bottom row). After considering all constraints, the “wrong sign” region from Figure 1 gets excluded by the direct

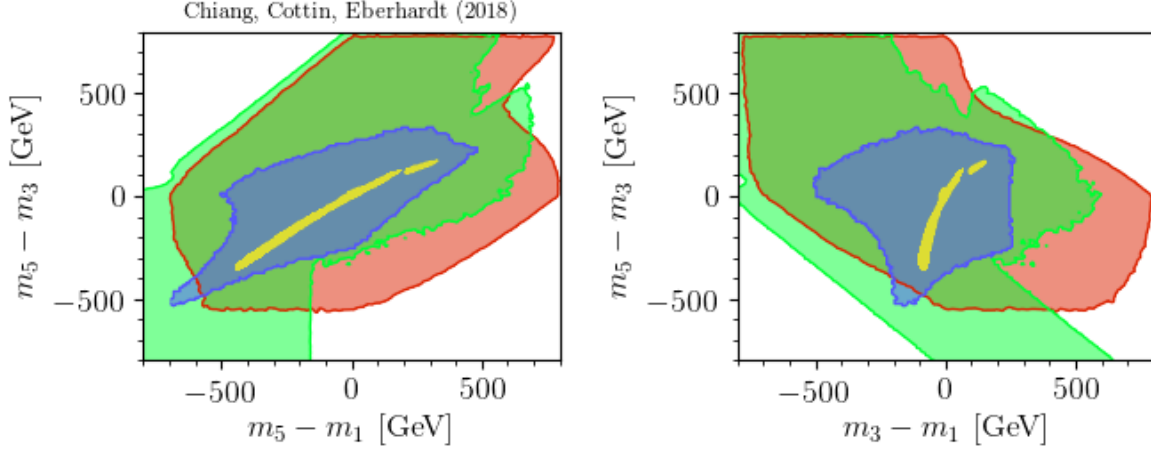
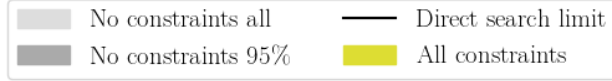


FIG. 3. Mass differences allowed at 95% probability. We show regions in the planes of $m_5 - m_1$ (left) and $m_3 - m_1$ (right) vs. $m_5 - m_3$. Effects of the theoretical constraints, Higgs signal strengths, and direct searches are shown in blue, red and green, respectively. The global fit with all constraints is shown in yellow.

searches. The effect of the direct searches pushes v_Δ further down to less than about 25 GeV in the combined fit. Note that the decoupling limit [120] ($\alpha, v_\Delta \approx 0$) is not favored in the fit due to the choice that our mass priors only go up to 1 TeV.

Looking at the plots in the bottom row, we note that the exclusion of the wrong sign limit comes from the H_5 searches. The effect comes mostly from the searches for the doubly charged $H_5^{\pm\pm}$. The suppression of v_Δ stems from H_5 and H_3 searches, where mostly experimental limits on the neutral H_3 constrain v_Δ for m_3 between 200 and 400 GeV. In the middle row of Figure 2, a rather constant region of α close to 0° is favored across the scanned mass range. Note the vertical green band in the α - m_1 plane around 250 GeV for direct searches is an effect of our implementation: for $|\alpha| > 12^\circ$, the branching ratio of $H_1 \rightarrow hh$ is above 90%, but this can only be counterbalanced by the negative results of direct searches a few GeV above 250 GeV because of the finite step size in our interpolation.

Figure 3 shows the effect of the theory bounds, h signal strengths, direct searches and all constraints on the mass differences. Again, the colored contours represent the allowed regions with 95% probability except for the theoretical constraints, for which we assume flat likelihoods. Hence, the 95% contours would only reflect on the priors, and the 100% contours are used for theory. Here we can see the power of the global fit. The individual sets of experimental constraints are not very strong in the $m_5 - m_3$ vs. $m_5 - m_1$ and $m_5 - m_3$ vs. $m_3 - m_1$ planes. The most dominant constraints come from the theoretical bounds, even though they still allow for a sizable region in the mass difference planes. However, once we combine the limits in the α - v_Δ plane from the LHC experiments with the theoretical conditions in the global fit, the region that survives at 95% shrinks to a thin strip for



Chiang, Cottin, Eberhardt (2018)

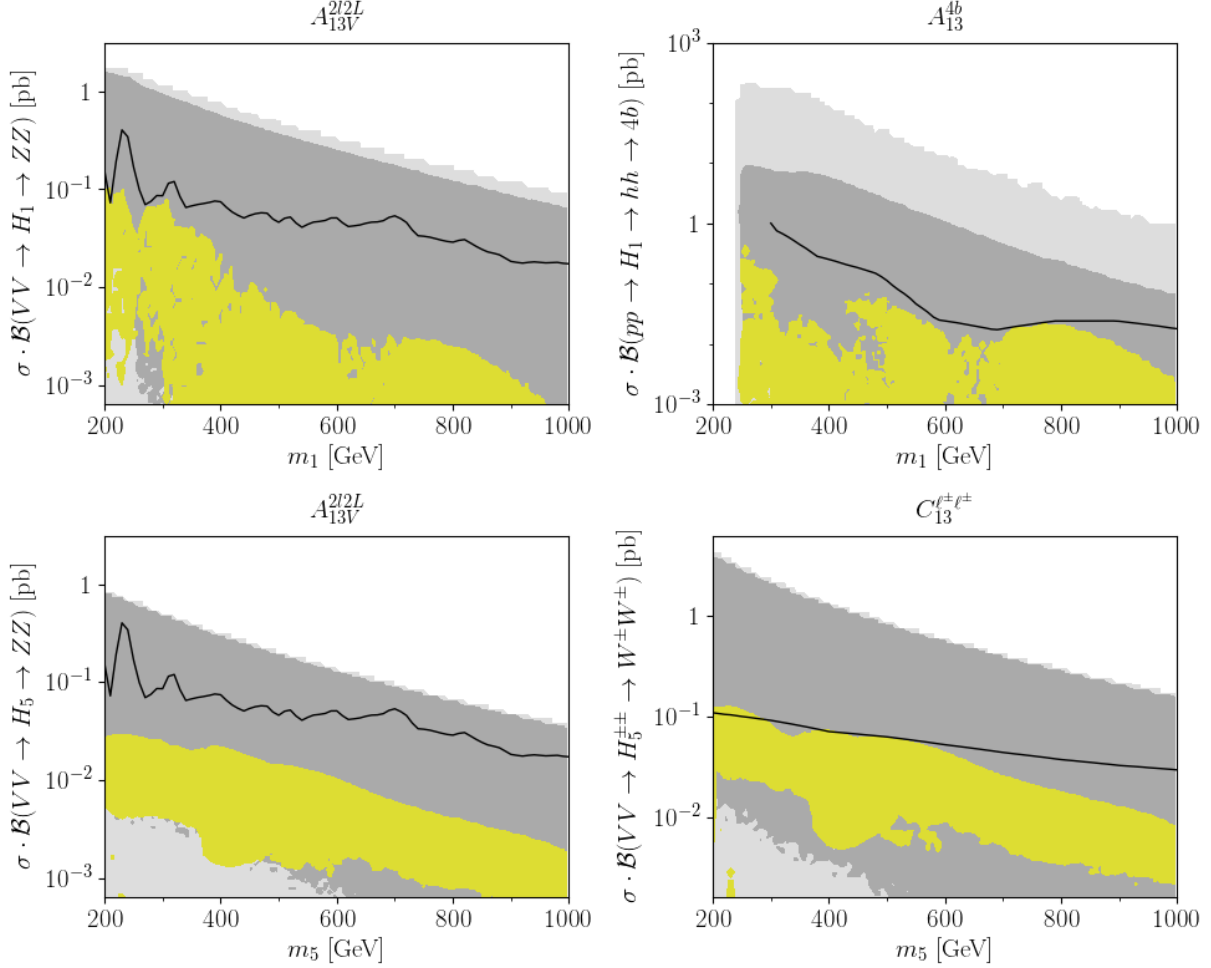


FIG. 4. Effect of three direct searches in the $\sigma \cdot \mathcal{B}$ vs. mass planes. The light (dark) grey regions show the 100% (95%) prior regions. The allowed 95% probability region after considering all the constraints is shown in yellow. The black curves denote the experimental limits on H_1 or H_5 decays to two Z bosons, on $H_1 \rightarrow hh$ and on the pair production of $H_5^{\pm\pm}$.

$|m_3 - m_1| < 200$ GeV (the yellow region). The disjoint regions at $m_5 - m_1 \approx 250$ GeV and $m_3 - m_1 \approx 120$ GeV are a consequence of our implementation of the direct searches: following Ref. [26], we only include on-shell decays of the H_5 bosons. With an increasing H_5 mass, the decay to a neutral or charged H_3 and a massive vector boson can open abruptly. For instance, the branching ratio of $H_5^0 \rightarrow H_3^0 Z$ can jump to values over 50%. If off-shell decays are also considered, then the transition for these decays becomes smooth, and the two regions should be connected.

Parameter	95% probability range	Parameter	95% probability range
v_Δ [GeV] $\cos\beta$	≤ 37 ≤ 0.43	λ_1	[0.03; 0.18]
α	$[-24^\circ; 1^\circ]$	λ_2	$[-0.6; 1.2]$
$m_5 - m_3$ [GeV]	$[-280; 180]$	λ_3	$[-1.1; 1.5]$
$m_5 - m_1$ [GeV]	$[-340; 350]$	λ_4	$[-0.21; 0.58]$
$m_3 - m_1$ [GeV]	$[-80; 170]$	λ_5	$[-2.7; 2.5]$

TABLE V. 95% probability intervals on the GM model parameters after considering all the constraints in our fits, marginalizing over all other parameters.

After considering all the direct searches from the previous section, we find that the most powerful experimental analyses in constraining this model involve searches for the H_1^0 and $H_5^{\pm\pm}$ bosons. The effect on H_3^0 and $H_{3,5}^\pm$ is not as strong. In order to give a closer insight into our treatment of the direct searches and also to help the experimental collaborations better appreciate which search channels are more relevant or useful to the model, we show in Figure 4 four of the most constraining searches for heavy scalar resonances implemented in this work. These include the ATLAS searches for $pp \rightarrow H_1^0 \rightarrow hh \rightarrow bbbb$ [99] (labeled A_{13}^{4b}), $VV \rightarrow H_{1,5}^0 \rightarrow ZZ$ [80] (labeled $A_{13V}^{2\ell 2L}$) and the CMS search $VV \rightarrow H_5^{\pm\pm} \rightarrow W^\pm W^\pm$ [119], labeled $C_{13}^{\ell^\pm \ell^\pm}$. The grey regions in the background delimit the available GM space if we do not apply any constraint in the fit. We show the 100% prior ranges, but also the 95% prior regions, which in the $H_1 \rightarrow hh$ case differ by about one order of magnitude in $\sigma \cdot \mathcal{B}$. All these four searches cut away a sizable portion of the allowed parameter space, ranging from a difference of less than one order of magnitude between the $H_5 \rightarrow ZZ$ search limit and the grey contour to more than two orders of magnitude in $\sigma \cdot \mathcal{B}$ for the searches of $H_1 \rightarrow hh$ and for the pair production of doubly charged scalars. Comparing this to the role of the individual searches in the global fit (yellow contour), we observe that the search in the left column is not quite relevant, while the channels in the right column yield the strongest constraint for m_1 between 500 and 800 GeV and for m_5 between 200 and 600 GeV, respectively.

We present in Table V the 95% probability ranges of the model parameters from our global fit. We do not get limits for the trilinear couplings μ_1 and μ_2 . The upper limit of 80 GeV on $m_1 - m_3$ enables us to exclude the decays $H_1 \rightarrow H_3^{0,+} H_3^{0,-}$, $H_1 \rightarrow H_3 Z$ as well as $H_1 \rightarrow H_3^+ W^-$ with a probability of 95%.

Limits on derived quantities such as total decay widths and branching ratios for the $H_{1,3,5}$ scalars are presented in Table VI. For the total decay widths of the heavy singlet, triplet and quintet particles, we observe that they cannot exceed 90 GeV, 44 GeV and 11 GeV, respectively. For the SM-like Higgs boson, we obtain a probability range on Γ_h between 3.9 and 4.5 MeV. These limits on the heavy Higgs decays serve as a guidance for the LHC experiments in the design of new searches for the scalars in the GM model.

VI. SUMMARY

We have performed global fits in the Georgi-Machacek model for the first time, making use of the `HEPfit` package and the latest experimental data. We consider constraints from both theory (stability of the scalar potential and perturbative unitarity) and LHC Higgs

H_1	95% prob. range	H_3	95% prob. range	H_5	95% prob. range
Γ_1	≤ 90 GeV	Γ_3	≤ 31 GeV	Γ_5	≤ 11 GeV
$\mathcal{B}(H_1^0 \rightarrow tt)$	[0;45] %	$\mathcal{B}(H_3^0 \rightarrow tt)$	[0;98] %	$\mathcal{B}(H_5^0 \rightarrow ZZ)$	[1;67] %
$\mathcal{B}(H_1^0 \rightarrow bb)$	[0;15] %	$\mathcal{B}(H_3^0 \rightarrow bb)$	[0;68] %	$\mathcal{B}(H_5^0 \rightarrow WW)$	[4;98] %
$\mathcal{B}(H_1^0 \rightarrow \tau\tau)$	[0;8] %	$\mathcal{B}(H_3^0 \rightarrow \tau\tau)$	[0;8] %	$\mathcal{B}(H_5^0 \rightarrow H_3 Z)$	[0;66] %
$\mathcal{B}(H_1^0 \rightarrow ZZ)$	[0;31] %	$\mathcal{B}(H_3^0 \rightarrow hZ)$	[0;100] %	$\mathcal{B}(H_5^0 \rightarrow H_3^+ W^-)$	[0;22] %
$\mathcal{B}(H_1^0 \rightarrow WW)$	[0;98] %	$\mathcal{B}(H_3^0 \rightarrow H_1 Z)$	[0;100] %	Γ_{5+} ≤ 11 GeV	
$\mathcal{B}(H_1^0 \rightarrow hh)$	[0;100] %	$\mathcal{B}(H_3^0 \rightarrow H_5 Z)$	[0;56] %	$\mathcal{B}(H_5^+ \rightarrow ZW^+)$	[10;100] %
$\mathcal{B}(H_1^0 \rightarrow H_5^0 H_5^0)$	[0;100] %	$\mathcal{B}(H_3^0 \rightarrow H_5^+ W^-)$	[0;99] %	$\mathcal{B}(H_5^+ \rightarrow H_3^+ Z)$	[0;41] %
		Γ_{3+} ≤ 44 GeV		$\mathcal{B}(H_5^+ \rightarrow H_3^0 W^+)$	[0;50] %
		$\mathcal{B}(H_3^+ \rightarrow tb)$	[0;100] %	Γ_{5++} ≤ 11 GeV	
		$\mathcal{B}(H_3^+ \rightarrow hW^+)$	[0;100] %	$\mathcal{B}(H_5^{++} \rightarrow W^+ W^+)$	[8;100] %
		$\mathcal{B}(H_3^+ \rightarrow H_1 W^+)$	[0;91] %	$\mathcal{B}(H_5^{++} \rightarrow H_3^+ W^+)$	[0;90] %
		$\mathcal{B}(H_3^+ \rightarrow H_5^+ Z)$	[0;29] %		
		$\mathcal{B}(H_3^+ \rightarrow H_5 W^+)$	[0;11] %		
		$\mathcal{B}(H_3^+ \rightarrow H_5^{++} W^-)$	[0;62] %		

TABLE VI. 95% probability intervals on the GM model decay widths and branching ratios after considering all constrains in our fits. We only quote branching ratios larger than 5%.

observables. These include several up-to-date experimental results from Run 1 and Run 2 of the LHC, including all the data on Higgs boson signal strengths and sixty-seven searches sensitive to the neutral, singly charged and doubly charged heavy Higgs particles of the Georgi-Machacek model.

By considering only the signal strengths for the SM-like Higgs boson, we have found a previously unexplored region in the v_Δ - α plane, featuring a negative sign in the Higgs couplings to vector bosons with respect to the SM couplings. This solution around $v_\Delta \approx 77$ GeV and $\alpha \approx 61^\circ$ cannot be ruled out by the signal strength data alone, but disappears as soon as direct search constraints are also imposed in the fit. The latter, especially the hunt for CP-even scalars, strongly constrains the vacuum expectation value of the Higgs triplet fields.

Combining the LHC bounds with the theory constraints in a global fit, we extract 95% probability limits on several Georgi-Machacek parameter regions and phenomenologically relevant quantities, which are significantly stronger than the bounds one would obtain when applying only one of the aforementioned sets of constraints. Among these are that α has to be between -24° and 1° and v_Δ smaller than 37 GeV. The latter means that $\cos \beta$ cannot exceed 0.43, which corresponds to an upper bound on $\sin \theta_H$, where the mixing angle θ_H is also used in the literature. We have found 95% limits on the differences between the heavy Higgs masses of values less than 350 GeV. The possibility of an H_1 decaying to H_3 can be excluded. We obtain upper 95% bounds on the total decay widths of the Higgs states and on many branching ratios. For instance, the $H_5^{\pm\pm}$ boson cannot decay into two H_3^\pm bosons.

The existence of a singly charged H_5^\pm and doubly charged $H_5^{\pm\pm}$ scalars is a distinctive feature of the Georgi-Machacek model. Ongoing searches at the LHC (see Table IV) directly constrain v_Δ . Current searches for $H_5^{\pm\pm}$ producing di-lepton resonances could also be useful

in constraining the Georgi-Machacek model in a global fit, which we did not consider in this work. This motivates flexibility in the definition of the experimental benchmarks in these searches to cases where the branching ratio of $H_5^{\pm\pm}$ to leptons is small, and its decay to vector bosons dominates.

ACKNOWLEDGMENTS

This research of C.-W. C. was supported in part by the Ministry of Science and Technology (MOST) of Taiwan under Grant No. MOST-104-2628-M-002-014-MY4. G.C. acknowledges support by Grant No. MOST-106-2811-M-002-035. This work has been supported in part by the Agencia Estatal de Investigación (AEI, ES) and the European Regional Development Fund (ERDF, EU) [Grants No. FPA2014-53631-C2-1-P, FPA2017-84445-P and SEV-2014-0398]. We thank Jorge de Blas for help with the Higgs signal strength inputs and Ayan Paul for his technical support with `HEPfit`. The fits were performed on the cluster of INFN Roma Tre.

-
- [1] ATLAS collaboration, G. Aad et al., *Observation of a new particle in the search for the Standard Model Higgs boson with the ATLAS detector at the LHC*, *Phys. Lett.* **B716** (2012) 1–29, [[1207.7214](#)].
 - [2] CMS collaboration, S. Chatrchyan et al., *Observation of a new boson at a mass of 125 GeV with the CMS experiment at the LHC*, *Phys. Lett.* **B716** (2012) 30–61, [[1207.7235](#)].
 - [3] PARTICLE DATA GROUP collaboration, C. Patrignani et al., *Review of Particle Physics*, *Chin. Phys.* **C40** (2016) 100001.
 - [4] H. Georgi and M. Machacek, *DOUBLY CHARGED HIGGS BOSONS*, *Nucl. Phys.* **B262** (1985) 463–477.
 - [5] M. S. Chanowitz and M. Golden, *Higgs Boson Triplets With $M(W) = M(Z) \cos \theta_W$* , *Phys. Lett.* **165B** (1985) 105–108.
 - [6] CMS collaboration, A. M. Sirunyan et al., *Measurements of properties of the Higgs boson decaying to a W boson pair in pp collisions at $\sqrt{s} = 13$ TeV*, [1806.05246](#).
 - [7] J. F. Gunion, R. Vega and J. Wudka, *Higgs triplets in the standard model*, *Phys. Rev.* **D42** (1990) 1673–1691.
 - [8] C.-W. Chiang, A.-L. Kuo and K. Yagyu, *Enhancements of weak gauge boson scattering processes at the CERN LHC*, *JHEP* **10** (2013) 072, [[1307.7526](#)].
 - [9] C.-W. Chiang, A.-L. Kuo and K. Yagyu, *Radiative corrections to Higgs couplings with weak gauge bosons in custodial multi-Higgs models*, *Phys. Lett.* **B774** (2017) 119–122, [[1707.04176](#)].
 - [10] C.-W. Chiang, A.-L. Kuo and K. Yagyu, *One-loop renormalized Higgs vertices in Georgi-Machacek model*, [1804.02633](#).
 - [11] C.-W. Chiang and K. Yagyu, *Testing the custodial symmetry in the Higgs sector of the Georgi-Machacek model*, *JHEP* **01** (2013) 026, [[1211.2658](#)].
 - [12] C.-W. Chiang, S. Kanemura and K. Yagyu, *Novel constraint on the parameter space of the Georgi-Machacek model with current LHC data*, *Phys. Rev.* **D90** (2014) 115025, [[1407.5053](#)].
 - [13] C.-W. Chiang and K. Tsumura, *Properties and searches of the exotic neutral Higgs bosons in the Georgi-Machacek model*, *JHEP* **04** (2015) 113, [[1501.04257](#)].

- [14] H. E. Logan and V. Rentala, *All the generalized Georgi-Machacek models*, *Phys. Rev.* **D92** (2015) 075011, [[1502.01275](#)].
- [15] C.-W. Chiang, A.-L. Kuo and T. Yamada, *Searches of exotic Higgs bosons in general mass spectra of the Georgi-Machacek model at the LHC*, *JHEP* **01** (2016) 120, [[1511.00865](#)].
- [16] C. Degrande, K. Hartling and H. E. Logan, *Scalar decays to $\gamma\gamma$, $Z\gamma$, and $W\gamma$ in the Georgi-Machacek model*, *Phys. Rev.* **D96** (2017) 075013, [[1708.08753](#)].
- [17] H. E. Logan and M. B. Reimer, *Characterizing a benchmark scenario for heavy Higgs boson searches in the Georgi-Machacek model*, *Phys. Rev.* **D96** (2017) 095029, [[1709.01883](#)].
- [18] “HEPfit Collaboration, HEPfit: a code for the combination of indirect and direct constraints on high energy physics models.” <http://hepfit.roma1.infn.it/>.
- [19] A. Caldwell, D. Kollar and K. Kroninger, *BAT: The Bayesian Analysis Toolkit*, *Comput. Phys. Commun.* **180** (2009) 2197–2209, [[0808.2552](#)].
- [20] V. Cacchio, D. Chowdhury, O. Eberhardt and C. W. Murphy, *Next-to-leading order unitarity fits in Two-Higgs-Doublet models with soft Z_2 breaking*, *JHEP* **11** (2016) 026, [[1609.01290](#)].
- [21] D. Chowdhury and O. Eberhardt, *Update of Global Two-Higgs-Doublet Model Fits*, *JHEP* **05** (2018) 161, [[1711.02095](#)].
- [22] O. Eberhardt, “Current status of two-higgs-doublet models with a softly broken z_2 symmetry.” ICHEP 2018 proceedings.
- [23] J. de Blas, M. Ciuchini, E. Franco, S. Mishima, M. Pierini, L. Reina et al., *Electroweak precision observables and Higgs-boson signal strengths in the Standard Model and beyond: present and future*, *JHEP* **12** (2016) 135, [[1608.01509](#)].
- [24] A. Arhrib, R. Benbrik, M. Chabab, G. Moulhaka, M. C. Peyranere, L. Rahili et al., *The Higgs Potential in the Type II Seesaw Model*, *Phys. Rev.* **D84** (2011) 095005, [[1105.1925](#)].
- [25] M. Aoki and S. Kanemura, *Unitarity bounds in the Higgs model including triplet fields with custodial symmetry*, *Phys. Rev.* **D77** (2008) 095009, [[0712.4053](#)].
- [26] K. Hartling, K. Kumar and H. E. Logan, *GM CALC: a calculator for the Georgi-Machacek model*, [1412.7387](#).
- [27] ATLAS collaboration, G. Aad et al., *Observation and measurement of Higgs boson decays to WW^* with the ATLAS detector*, *Phys. Rev.* **D92** (2015) 012006, [[1412.2641](#)].
- [28] CMS collaboration, S. Chatrchyan et al., *Measurement of Higgs boson production and properties in the WW decay channel with leptonic final states*, *JHEP* **01** (2014) 096, [[1312.1129](#)].
- [29] ATLAS collaboration, G. Aad et al., *Evidence for the Higgs-boson Yukawa coupling to tau leptons with the ATLAS detector*, *JHEP* **04** (2015) 117, [[1501.04943](#)].
- [30] CMS collaboration, S. Chatrchyan et al., *Evidence for the 125 GeV Higgs boson decaying to a pair of τ leptons*, *JHEP* **05** (2014) 104, [[1401.5041](#)].
- [31] ATLAS collaboration, G. Aad et al., *Measurements of Higgs boson production and couplings in the four-lepton channel in pp collisions at center-of-mass energies of 7 and 8 TeV with the ATLAS detector*, *Phys. Rev.* **D91** (2015) 012006, [[1408.5191](#)].
- [32] CMS collaboration, V. Khachatryan et al., *Precise determination of the mass of the Higgs boson and tests of compatibility of its couplings with the standard model predictions using proton collisions at 7 and 8 TeV*, *Eur. Phys. J.* **C75** (2015) 212, [[1412.8662](#)].
- [33] ATLAS collaboration, G. Aad et al., *Measurement of Higgs boson production in the diphoton decay channel in pp collisions at center-of-mass energies of 7 and 8 TeV with the ATLAS detector*, *Phys. Rev.* **D90** (2014) 112015, [[1408.7084](#)].
- [34] CMS collaboration, V. Khachatryan et al., *Observation of the diphoton decay of the Higgs*

- boson and measurement of its properties*, *Eur. Phys. J.* **C74** (2014) 3076, [[1407.0558](#)].
- [35] ATLAS collaboration, G. Aad et al., *Measurements of the Higgs boson production and decay rates and coupling strengths using pp collision data at $\sqrt{s} = 7$ and 8 TeV in the ATLAS experiment*, *Eur. Phys. J.* **C76** (2016) 6, [[1507.04548](#)].
 - [36] ATLAS, CMS collaboration, G. Aad et al., *Measurements of the Higgs boson production and decay rates and constraints on its couplings from a combined ATLAS and CMS analysis of the LHC pp collision data at $\sqrt{s} = 7$ and 8 TeV*, *JHEP* **08** (2016) 045, [[1606.02266](#)].
 - [37] ATLAS collaboration, *Measurement of gluon fusion and vector boson fusion Higgs boson production cross-sections in the $H \rightarrow WW^* \rightarrow e\nu\mu\nu$ decay channel in pp collisions at $\sqrt{s} = 13$ TeV with the ATLAS detector*, Tech. Rep. ATLAS-CONF-2018-004, CERN, Geneva, Mar, 2018.
 - [38] CMS collaboration, A. M. Sirunyan et al., *Observation of the Higgs boson decay to a pair of τ leptons with the CMS detector*, *Phys. Lett.* **B779** (2018) 283–316, [[1708.00373](#)].
 - [39] ATLAS collaboration, M. Aaboud et al., *Measurement of the Higgs boson coupling properties in the $H \rightarrow ZZ^* \rightarrow 4\ell$ decay channel at $\sqrt{s} = 13$ TeV with the ATLAS detector*, *JHEP* **03** (2018) 095, [[1712.02304](#)].
 - [40] CMS collaboration, A. M. Sirunyan et al., *Measurements of properties of the Higgs boson decaying into the four-lepton final state in pp collisions at $\sqrt{s} = 13$ TeV*, *JHEP* **11** (2017) 047, [[1706.09936](#)].
 - [41] ATLAS collaboration, M. Aaboud et al., *Measurements of Higgs boson properties in the diphoton decay channel with 36 fb^{-1} of pp collision data at $\sqrt{s} = 13$ TeV with the ATLAS detector*, [1802.04146](#).
 - [42] CMS collaboration, A. M. Sirunyan et al., *Measurements of Higgs boson properties in the diphoton decay channel in proton-proton collisions at $\sqrt{s} = 13$ TeV*, [1804.02716](#).
 - [43] CMS collaboration, A. M. Sirunyan et al., *Search for the decay of a Higgs boson in the $\ell\ell\gamma$ channel in proton-proton collisions at $\sqrt{s} = 13$ TeV*, [1806.05996](#).
 - [44] ATLAS collaboration, M. Aaboud et al., *Search for the dimuon decay of the Higgs boson in pp collisions at $\sqrt{s} = 13$ TeV with the ATLAS detector*, *Phys. Rev. Lett.* **119** (2017) 051802, [[1705.04582](#)].
 - [45] CMS collaboration, *Search for the standard model Higgs boson decaying into two muons in pp collisions at $\sqrt{s}=13\text{TeV}$* , Tech. Rep. CMS-PAS-HIG-17-019, CERN, Geneva, 2017.
 - [46] CMS collaboration, *Search for the standard model Higgs boson produced through vector boson fusion and decaying to $b\bar{b}$ with proton-proton collisions at $\sqrt{s} = 13$ TeV*, Tech. Rep. CMS-PAS-HIG-16-003, CERN, Geneva, 2016.
 - [47] ATLAS collaboration, G. Aad et al., *Search for the $b\bar{b}$ decay of the Standard Model Higgs boson in associated (W/Z)H production with the ATLAS detector*, *JHEP* **01** (2015) 069, [[1409.6212](#)].
 - [48] CMS collaboration, S. Chatrchyan et al., *Search for the standard model Higgs boson produced in association with a W or a Z boson and decaying to bottom quarks*, *Phys. Rev.* **D89** (2014) 012003, [[1310.3687](#)].
 - [49] ATLAS collaboration, G. Aad et al., *Study of (W/Z)H production and Higgs boson couplings using $H \rightarrow WW^*$ decays with the ATLAS detector*, *JHEP* **08** (2015) 137, [[1506.06641](#)].
 - [50] ATLAS collaboration, M. Aaboud et al., *Evidence for the $H \rightarrow b\bar{b}$ decay with the ATLAS detector*, *JHEP* **12** (2017) 024, [[1708.03299](#)].
 - [51] CMS collaboration, A. M. Sirunyan et al., *Evidence for the Higgs boson decay to a bottom*

- quark?antiquark pair, *Phys. Lett.* **B780** (2018) 501–532, [[1709.07497](#)].
- [52] ATLAS collaboration, *Measurements of the Higgs boson production cross section via Vector Boson Fusion and associated WH production in the $WW^* \rightarrow \ell\nu\ell\nu$ decay mode with the ATLAS detector at $\sqrt{s} = 13$ TeV*, Tech. Rep. ATLAS-CONF-2016-112, CERN, Geneva, Nov, 2016.
 - [53] ATLAS collaboration, G. Aad et al., *Search for the Standard Model Higgs boson produced in association with top quarks and decaying into $b\bar{b}$ in pp collisions at $\sqrt{s} = 8$ TeV with the ATLAS detector*, *Eur. Phys. J.* **C75** (2015) 349, [[1503.05066](#)].
 - [54] CMS collaboration, V. Khachatryan et al., *Search for the associated production of the Higgs boson with a top-quark pair*, *JHEP* **09** (2014) 087, [[1408.1682](#)].
 - [55] ATLAS collaboration, M. Aaboud et al., *Search for the standard model Higgs boson produced in association with top quarks and decaying into a $b\bar{b}$ pair in pp collisions at $\sqrt{s} = 13$ TeV with the ATLAS detector*, *Phys. Rev.* **D97** (2018) 072016, [[1712.08895](#)].
 - [56] CMS collaboration, A. M. Sirunyan et al., *Search for $t\bar{t}H$ production in the all-jet final state in proton-proton collisions at $\sqrt{s} = 13$ TeV*, [1803.06986](#).
 - [57] CMS collaboration, A. M. Sirunyan et al., *Search for $t\bar{t}H$ production in the $H \rightarrow b\bar{b}$ decay channel with leptonic $t\bar{t}$ decays in proton-proton collisions at $\sqrt{s} = 13$ TeV*, [1804.03682](#).
 - [58] ATLAS collaboration, M. Aaboud et al., *Evidence for the associated production of the Higgs boson and a top quark pair with the ATLAS detector*, *Phys. Rev.* **D97** (2018) 072003, [[1712.08891](#)].
 - [59] CMS collaboration, A. M. Sirunyan et al., *Evidence for associated production of a Higgs boson with a top quark pair in final states with electrons, muons, and hadronically decaying τ leptons at $\sqrt{s} = 13$ TeV*, [1803.05485](#).
 - [60] CDF collaboration, T. Aaltonen et al., *Combination of Searches for the Higgs Boson Using the Full CDF Data Set*, *Phys. Rev.* **D88** (2013) 052013, [[1301.6668](#)].
 - [61] D0 collaboration, V. M. Abazov et al., *Combined search for the Higgs boson with the D0 experiment*, *Phys. Rev.* **D88** (2013) 052011, [[1303.0823](#)].
 - [62] J. de Blas, O. Eberhardt and C. Krause, *Current and Future Constraints on Higgs Couplings in the Nonlinear Effective Theory*, [1803.00939](#).
 - [63] ATLAS collaboration, *Search for new phenomena in $t\bar{t}$ final states with additional heavy-flavour jets in pp collisions at $\sqrt{s} = 13$ TeV with the ATLAS detector*, Tech. Rep. ATLAS-CONF-2016-104, CERN, Geneva, Sep, 2016.
 - [64] CMS collaboration, V. Khachatryan et al., *Search for Neutral MSSM Higgs Bosons Decaying into A Pair of Bottom Quarks*, *JHEP* **11** (2015) 071, [[1506.08329](#)].
 - [65] CMS collaboration, A. M. Sirunyan et al., *Search for narrow resonances in the b-tagged dijet mass spectrum in proton-proton collisions at $\sqrt{s} = 8$ TeV*, [1802.06149](#).
 - [66] CMS collaboration, *Search for a narrow heavy decaying to bottom quark pairs in the 13 TeV data sample*, Tech. Rep. CMS-PAS-HIG-16-025, CERN, Geneva, 2016.
 - [67] CMS collaboration, *Search for Higgs bosons produced in association with b quarks and decaying into a b-quark pair with 13 TeV data*, Tech. Rep. CMS-PAS-HIG-16-018, CERN, Geneva, 2018.
 - [68] ATLAS collaboration, G. Aad et al., *Search for neutral Higgs bosons of the minimal supersymmetric standard model in pp collisions at $\sqrt{s} = 8$ TeV with the ATLAS detector*, *JHEP* **11** (2014) 056, [[1409.6064](#)].
 - [69] CMS collaboration, *Search for additional neutral Higgs bosons decaying to a pair of tau leptons in pp collisions at $\sqrt{s} = 7$ and 8 TeV*, Tech. Rep. CMS-PAS-HIG-14-029, CERN,

- Geneva, 2015.
- [70] ATLAS collaboration, M. Aaboud et al., *Search for additional heavy neutral Higgs and gauge bosons in the ditau final state produced in 36 fb^{-1} of pp collisions at $\sqrt{s} = 13 \text{ TeV}$ with the ATLAS detector*, *JHEP* **01** (2018) 055, [[1709.07242](#)].
 - [71] CMS collaboration, A. M. Sirunyan et al., *Search for additional neutral MSSM Higgs bosons in the $\tau\tau$ final state in proton-proton collisions at $\sqrt{s} = 13 \text{ TeV}$* , [1803.06553](#).
 - [72] ATLAS collaboration, G. Aad et al., *Search for Scalar Diphoton Resonances in the Mass Range $65 - 600 \text{ GeV}$ with the ATLAS Detector in pp Collision Data at $\sqrt{s} = 8 \text{ TeV}$* , *Phys. Rev. Lett.* **113** (2014) 171801, [[1407.6583](#)].
 - [73] ATLAS collaboration, M. Aaboud et al., *Search for new phenomena in high-mass diphoton final states using 37 fb^{-1} of proton-proton collisions collected at $\sqrt{s} = 13 \text{ TeV}$ with the ATLAS detector*, *Phys. Lett.* **B775** (2017) 105–125, [[1707.04147](#)].
 - [74] CMS collaboration, V. Khachatryan et al., *Search for high-mass diphoton resonances in proton-proton collisions at 13 TeV and combination with 8 TeV search*, *Phys. Lett.* **B767** (2017) 147–170, [[1609.02507](#)].
 - [75] ATLAS collaboration, G. Aad et al., *Search for new resonances in $W\gamma$ and $Z\gamma$ final states in pp collisions at $\sqrt{s} = 8 \text{ TeV}$ with the ATLAS detector*, *Phys. Lett.* **B738** (2014) 428–447, [[1407.8150](#)].
 - [76] CMS collaboration, *Search for scalar resonances in the $200\text{--}1200 \text{ GeV}$ mass range decaying into a Z and a photon in pp collisions at $\sqrt{s} = 8 \text{ TeV}$* , Tech. Rep. CMS-PAS-HIG-16-014, CERN, Geneva, 2016.
 - [77] ATLAS collaboration, M. Aaboud et al., *Searches for the $Z\gamma$ decay mode of the Higgs boson and for new high-mass resonances in pp collisions at $\sqrt{s} = 13 \text{ TeV}$ with the ATLAS detector*, *JHEP* **10** (2017) 112, [[1708.00212](#)].
 - [78] CMS collaboration, A. M. Sirunyan et al., *Search for $Z\gamma$ resonances using leptonic and hadronic final states in proton-proton collisions at $\sqrt{s} = 13 \text{ TeV}$* , [1712.03143](#).
 - [79] ATLAS collaboration, G. Aad et al., *Search for an additional, heavy Higgs boson in the $H \rightarrow ZZ$ decay channel at $\sqrt{s} = 8 \text{ TeV}$ in pp collision data with the ATLAS detector*, *Eur. Phys. J.* **C76** (2016) 45, [[1507.05930](#)].
 - [80] ATLAS collaboration, M. Aaboud et al., *Search for heavy ZZ resonances in the $\ell^+\ell^-\ell^+\ell^-$ and $\ell^+\ell^-\nu\bar{\nu}$ final states using proton proton collisions at $\sqrt{s} = 13 \text{ TeV}$ with the ATLAS detector*, [1712.06386](#).
 - [81] ATLAS collaboration, M. Aaboud et al., *Searches for heavy ZZ and ZW resonances in the $\ell\ell q\bar{q}$ and $\nu\nu q\bar{q}$ final states in pp collisions at $\sqrt{s} = 13 \text{ TeV}$ with the ATLAS detector*, [1708.09638](#).
 - [82] CMS collaboration, A. M. Sirunyan et al., *Search for a new scalar resonance decaying to a pair of Z bosons in proton-proton collisions at $\sqrt{s} = 13 \text{ TeV}$* , [1804.01939](#).
 - [83] ATLAS collaboration, G. Aad et al., *Search for a high-mass Higgs boson decaying to a W boson pair in pp collisions at $\sqrt{s} = 8 \text{ TeV}$ with the ATLAS detector*, *JHEP* **01** (2016) 032, [[1509.00389](#)].
 - [84] ATLAS collaboration, M. Aaboud et al., *Search for heavy resonances decaying into WW in the $e\nu\mu\nu$ final state in pp collisions at $\sqrt{s} = 13 \text{ TeV}$ with the ATLAS detector*, *Eur. Phys. J.* **C78** (2018) 24, [[1710.01123](#)].
 - [85] CMS collaboration, *Search for high mass Higgs to WW with fully leptonic decays using 2015 data*, Tech. Rep. CMS-PAS-HIG-16-023, CERN, Geneva, 2016.
 - [86] ATLAS collaboration, M. Aaboud et al., *Search for WW/WZ resonance production in*

- $\ell\nu q\bar{q}$ final states in pp collisions at $\sqrt{s} = 13$ TeV with the ATLAS detector*, [1710.07235](#).
- [87] CMS collaboration, V. Khachatryan et al., *Search for a Higgs Boson in the Mass Range from 145 to 1000 GeV Decaying to a Pair of W or Z Bosons*, *JHEP* **10** (2015) 144, [[1504.00936](#)].
 - [88] CMS collaboration, S. Chatrchyan et al., *A search for a doubly-charged Higgs boson in pp collisions at $\sqrt{s} = 7$ TeV*, *Eur. Phys. J.* **C72** (2012) 2189, [[1207.2666](#)].
 - [89] CMS collaboration, *Search for a doubly-charged Higgs boson with $\sqrt{s} = 8$ TeV pp collisions at the CMS experiment*, Tech. Rep. CMS-PAS-HIG-14-039, CERN, Geneva, 2016.
 - [90] CMS collaboration, *A search for doubly-charged Higgs boson production in three and four lepton final states at $\sqrt{s} = 13$ TeV*, Tech. Rep. CMS-PAS-HIG-16-036, CERN, Geneva, 2017.
 - [91] ATLAS collaboration, G. Aad et al., *Search for anomalous production of prompt same-sign lepton pairs and pair-produced doubly charged Higgs bosons with $\sqrt{s} = 8$ TeV pp collisions using the ATLAS detector*, *JHEP* **03** (2015) 041, [[1412.0237](#)].
 - [92] ATLAS collaboration, M. Aaboud et al., *Search for doubly charged Higgs boson production in multi-lepton final states with the ATLAS detector using proton-proton collisions at $\sqrt{s} = 13$ TeV*, [1710.09748](#).
 - [93] S. Kanemura, M. Kikuchi, H. Yokoya and K. Yagyu, *LHC Run-I constraint on the mass of doubly charged Higgs bosons in the same-sign diboson decay scenario*, *PTEP* **2015** (2015) 051B02, [[1412.7603](#)].
 - [94] ATLAS collaboration, G. Aad et al., *Searches for Higgs boson pair production in the $hh \rightarrow b\bar{b}\tau\tau, \gamma\gamma WW^*, \gamma\gamma b\bar{b}, b\bar{b}b\bar{b}$ channels with the ATLAS detector*, *Phys. Rev.* **D92** (2015) 092004, [[1509.04670](#)].
 - [95] CMS collaboration, V. Khachatryan et al., *Search for resonant pair production of Higgs bosons decaying to two bottom quark-antiquark pairs in proton-proton collisions at 8 TeV*, *Phys. Lett.* **B749** (2015) 560–582, [[1503.04114](#)].
 - [96] CMS collaboration, V. Khachatryan et al., *Search for two Higgs bosons in final states containing two photons and two bottom quarks in proton-proton collisions at 8 TeV*, *Phys. Rev.* **D94** (2016) 052012, [[1603.06896](#)].
 - [97] CMS collaboration, V. Khachatryan et al., *Searches for a heavy scalar boson H decaying to a pair of 125 GeV Higgs bosons hh or for a heavy pseudoscalar boson A decaying to Zh , in the final states with $h \rightarrow \tau\tau$* , *Phys. Lett.* **B755** (2016) 217–244, [[1510.01181](#)].
 - [98] CMS collaboration, A. M. Sirunyan et al., *Search for Higgs boson pair production in the $b\bar{b}\tau\tau$ final state in proton-proton collisions at $\sqrt{s} = 8$ TeV*, *Phys. Rev.* **D96** (2017) 072004, [[1707.00350](#)].
 - [99] ATLAS collaboration, *Search for pair production of Higgs bosons in the $b\bar{b}b\bar{b}$ final state using proton-proton collisions at $\sqrt{s} = 13$ TeV with the ATLAS detector*, Tech. Rep. ATLAS-CONF-2016-049, CERN, Geneva, Aug, 2016.
 - [100] CMS collaboration, *Search for resonant pair production of Higgs bosons decaying to bottom quark-antiquark pairs in proton-proton collisions at 13 TeV*, Tech. Rep. CMS-PAS-HIG-17-009, CERN, Geneva, 2017.
 - [101] ATLAS collaboration, *Search for Higgs boson pair production in the $b\bar{b}\gamma\gamma$ final state using pp collision data at $\sqrt{s} = 13$ TeV with the ATLAS detector*, Tech. Rep. ATLAS-CONF-2016-004, CERN, Geneva, Mar, 2016.
 - [102] CMS collaboration, A. M. Sirunyan et al., *Search for Higgs boson pair production in the $\gamma\gamma b\bar{b}$ final state in pp collisions at $\sqrt{s} = 13$ TeV*, [1806.00408](#).
 - [103] CMS collaboration, A. M. Sirunyan et al., *Search for Higgs boson pair production in events*

- with two bottom quarks and two tau leptons in proton-proton collisions at $\sqrt{s} = 13 \text{ TeV}$, *Phys. Lett. B* **778** (2018) 101–127, [[1707.02909](#)].
- [104] CMS collaboration, A. M. Sirunyan et al., *Search for resonant and nonresonant Higgs boson pair production in the $b\bar{b}l\nu l\nu$ final state in proton-proton collisions at $\sqrt{s} = 13 \text{ TeV}$* , [1708.04188](#).
 - [105] ATLAS collaboration, *Search for Higgs boson pair production in the final state of $\gamma\gamma WW^*(\rightarrow l\nu jj)$ using 13.3 fb^{-1} of pp collision data recorded at $\sqrt{s} = 13 \text{ TeV}$ with the ATLAS detector*, Tech. Rep. ATLAS-CONF-2016-071, CERN, Geneva, Aug, 2016.
 - [106] ATLAS collaboration, G. Aad et al., *Search for a CP -odd Higgs boson decaying to Zh in pp collisions at $\sqrt{s} = 8 \text{ TeV}$ with the ATLAS detector*, *Phys. Lett. B* **744** (2015) 163–183, [[1502.04478](#)].
 - [107] CMS collaboration, V. Khachatryan et al., *Search for a pseudoscalar boson decaying into a Z boson and the 125 GeV Higgs boson in $\ell^+\ell^-\bar{b}b$ final states*, *Phys. Lett. B* **748** (2015) 221–243, [[1504.04710](#)].
 - [108] ATLAS collaboration, M. Aaboud et al., *Search for heavy resonances decaying into a W or Z boson and a Higgs boson in final states with leptons and b -jets in 36 fb^{-1} of $\sqrt{s} = 13 \text{ TeV}$ pp collisions with the ATLAS detector*, [1712.06518](#).
 - [109] CMS collaboration, V. Khachatryan et al., *Search for neutral resonances decaying into a Z boson and a pair of b jets or τ leptons*, *Phys. Lett. B* **759** (2016) 369–394, [[1603.02991](#)].
 - [110] ATLAS collaboration, G. Aad et al., *Search for charged Higgs bosons decaying via $H^\pm \rightarrow \tau^\pm \nu$ in fully hadronic final states using pp collision data at $\sqrt{s} = 8 \text{ TeV}$ with the ATLAS detector*, *JHEP* **03** (2015) 088, [[1412.6663](#)].
 - [111] CMS collaboration, V. Khachatryan et al., *Search for a charged Higgs boson in pp collisions at $\sqrt{s} = 8 \text{ TeV}$* , *JHEP* **11** (2015) 018, [[1508.07774](#)].
 - [112] ATLAS collaboration, *Search for charged Higgs bosons in the τ +jets final state using 14.7 fb^{-1} of pp collision data recorded at $\sqrt{s} = 13 \text{ TeV}$ with the ATLAS experiment*, Tech. Rep. ATLAS-CONF-2016-088, CERN, Geneva, Aug, 2016.
 - [113] CMS collaboration, *Search for charged Higgs bosons with the $H^\pm \rightarrow \tau^\pm \nu_\tau$ decay channel in the fully hadronic final state at $\sqrt{s} = 13 \text{ TeV}$* , Tech. Rep. CMS-PAS-HIG-16-031, CERN, Geneva, 2016.
 - [114] ATLAS collaboration, G. Aad et al., *Search for charged Higgs bosons in the $H^\pm \rightarrow tb$ decay channel in pp collisions at $\sqrt{s} = 8 \text{ TeV}$ using the ATLAS detector*, *JHEP* **03** (2016) 127, [[1512.03704](#)].
 - [115] ATLAS collaboration, *Search for charged Higgs bosons in the $H^\pm \rightarrow tb$ decay channel in pp collisions at $\sqrt{s} = 13 \text{ TeV}$ using the ATLAS detector*, Tech. Rep. ATLAS-CONF-2016-089, CERN, Geneva, Aug, 2016.
 - [116] ATLAS collaboration, G. Aad et al., *Search for a Charged Higgs Boson Produced in the Vector-Boson Fusion Mode with Decay $H^\pm \rightarrow W^\pm Z$ using pp Collisions at $\sqrt{s} = 8 \text{ TeV}$ with the ATLAS Experiment*, *Phys. Rev. Lett.* **114** (2015) 231801, [[1503.04233](#)].
 - [117] CMS collaboration, A. M. Sirunyan et al., *Search for Charged Higgs Bosons Produced via Vector Boson Fusion and Decaying into a Pair of W and Z Bosons Using pp Collisions at $\sqrt{s} = 13 \text{ TeV}$* , *Phys. Rev. Lett.* **119** (2017) 141802, [[1705.02942](#)].
 - [118] CMS collaboration, V. Khachatryan et al., *Study of vector boson scattering and search for new physics in events with two same-sign leptons and two jets*, *Phys. Rev. Lett.* **114** (2015) 051801, [[1410.6315](#)].
 - [119] CMS collaboration, A. M. Sirunyan et al., *Observation of electroweak production of*

- same-sign W boson pairs in the two jet and two same-sign lepton final state in proton-proton collisions at $\sqrt{s} = 13$ TeV*, *Phys. Rev. Lett.* **120** (2018) 081801, [[1709.05822](#)].
- [120] K. Hartling, K. Kumar and H. E. Logan, *The decoupling limit in the Georgi-Machacek model*, *Phys. Rev.* **D90** (2014) 015007, [[1404.2640](#)].
- [121] “LHC Higgs Cross Section Working Group Collaboration, webpage.”
<https://twiki.cern.ch/twiki/bin/view/LHCPhysics/LHCHXSWG>.
- [122] J. Alwall, R. Frederix, S. Frixione, V. Hirschi, F. Maltoni, O. Mattelaer et al., *The automated computation of tree-level and next-to-leading order differential cross sections, and their matching to parton shower simulations*, *JHEP* **07** (2014) 079, [[1405.0301](#)].